Final version published as: Lira-Navarrete, E., Iglesias-Fernández, J., Zandberg, W. F., Compañón, I., Kong, Y., Corzana, F., Pinto, B. M., Clausen, H., Peregrina, J. M., Vocadlo, D. J., Rovira, C., & Hurtado-Guerrero, R. (2014). Substrate-Guided Front-Face Reaction Revealed by Combined Structural Snapshots and Metadynamics for the Polypeptide N-Acetylgalactosaminyltransferase 2. Angewandte Chemie International Edition, 53(31), 8206–8210. https://doi.org/10.1002/anie.201402781

Substrate-Guided Front-Face Reaction Revealed by Combined Structural Snapshots and Metadynamics for the Polypeptide *N*-Acetylgalactosaminyltransferase 2**

Erandi Lira-Navarrete, Javier Iglesias-Fernández, Wesley F. Zandberg, Ismael Compañón, Yun Kong, Francisco Corzana, B. Mario Pinto, Henrik Clausen, Jesús M. Peregrina, David J. Vocadlo, Carme Rovira, and Ramon Hurtado-Guerrero**

Abstract: *The retaining glycosyltransferase GalNAc-T2 is a member of a large family of human polypeptide GalNAc-transferases that is responsible for the post-translational modification of many cell-surface proteins. By the use of combined structural and computational approaches, we provide the first set of structural snapshots of the enzyme during the catalytic cycle and combine these with quantum-mechanics/molecular-mechanics (QM/MM) metadynamics to unravel the catalytic mechanism of this retaining enzyme at the atomic-electronic level of detail. Our study provides a detailed structural rationale for an ordered bi–bi kinetic mechanism and reveals critical aspects of substrate recognition, which dictate the specificity for acceptor Thr versus Ser residues and enforce a front-face S_Ni-type reaction in which the substrate N-acetyl sugar substituent coordinates efficient glycosyl transfer.*

O-GalNAc glycosylation[1] is by far the most complex and differentially regulated type of protein glycosylation, and it may also be the most abundant, with over 80% of all proteins passing through the secretory pathway predicted to be O-glycosylated.[2] One of the key enzyme isoforms that control human protein O-glycosylation is polypeptide GalNAc-transferase 2 (GalNAc-T2). This enzyme is part of a large family of retaining isoenzymes that transfer a GalNAc residue from UDP-GalNAc to Ser/Thr side chains and thereby initiate mucin-type or GalNAc-type protein O-glycosylation. How GalNAc-Ts target specific sites on proteins and glycoproteins, and how they catalyze O-GalNAc transfer is not understood. Although the structures of several GalNAc-Ts have been reported,[3] the lack of Michaelis complexes and ternary product complexes has limited mechanistic insight into the glycosyl-transfer reaction. Such information is required for the rational design of inhibitors of these potential drug targets.

Herein we describe the use of a combination of X-ray crystallography and quantum-mechanics/molecular-mechanics (QM/MM) metadynamics to unravel the catalytic mechanism of GalNAc-T2. The structures obtained provide the first structural snapshots of the enzyme in complex with its substrates and products during the catalytic cycle. The findings reveal mobile loops that act to bind and release the substrates and illuminate substrate acceptor preference for threonine over serine. Furthermore, QM/MM metadynamics simulations reveal a front-face reaction mechanism involving a short-lived oxocarbenium-ion-like intermediate.

To obtain a Michaelis complex of GalNAc-T2, we obtained crystals of GalNAc-T2 in complex with UDP-Mn^{2+} (UDP = uridine diphosphate) and soaked them first in

[*] E. Lira-Navarrete,[+] Dr. R. Hurtado-Guerrero
Institute of Biocomputation and Physics of Complex Systems (BIFI)
University of Zaragoza, BIFI-IQFR (CSIC) Joint Unit
Mariano Esquillor s/n, Campus Rio Ebro, Edificio I + D
Fundacion ARAID, Edificio Pignatelli 36 (Spain)
E-mail: rhurtado@bifi.es

J. Iglesias-Fernández,[+] Prof. C. Rovira
Departament de Química Orgànica and Institut de Química Teòrica i Computacional (IQTCUB), Universitat de Barcelona
Martí i Franquès 1, Barcelona (Spain)
E-mail: c.rovira@ub.edu

Prof. C. Rovira
Institució Catalana de Recerca i Estudis Avançats (ICREA)
Passeig Lluís Companys 23, 08020 Barcelona (Spain)

Dr. W. F. Zandberg, Prof. B. M. Pinto, Prof. D. J. Vocadlo
Department of Chemistry and Department of Molecular Biology and Biochemistry, Simon Fraser University, Burnaby, BC (Canada)

I. Compañón, Dr. F. Corzana, Prof. J. M. Peregrina
Departamento de Química, Universidad de La Rioja
Centro de Investigación en Síntesis Química, Logroño (Spain)

Y. Kong, Prof. H. Clausen
Copenhagen Center for Glycomics, Departments of Cellular and Molecular Medicine and School of Dentistry
University of Copenhagen (Denmark)

[+] These authors contributed equally.

[**] We thank the Diamond Light Source (DLS) at Oxford, in particular for the use of beamlines ID24 (experiment number MX8035-14) and I04-1 (experiment number MX8035-17). We thank the Fundación Agencia Aragonesa para la Investigación y el Desarrollo (ARAID, Spain), the Ministerio de Economía y Competitividad (MEC, Spain, grants BFU2010-19504 and CTQ2011-25871), The Danish National Research Foundation (DNRF107), the Diputación General de Aragón (Grupo Protein Targets, B89), and the Generalitat de Catalunya (2009SGR-1309). We acknowledge the computer support, technical expertise, and assistance provided by the Barcelona Supercomputing Center—Centro Nacional de Supercomputación (BSC-CNS). Funding for the research leading to these results was also received from the Seventh Framework Programme (FP7/2007-2013) of the European Community under BioStruct-X (grant agreement No. 283570), and the Natural Sciences and Engineering Research Council of Canada.

a solution containing UDP-GalNAc and subsequently with the EA2 acceptor peptide (sequence DST*T*PAPTTK, in which *T* is the predominant glycosylation site). The resulting crystals diffracted fairly well, thus enabling the structure to be solved at 2.45 Å (see Table S1 in the Supporting Information). Six molecules of GalNAc-T2 are arranged in three independent dimers (see Figure S1 in the Supporting Information) within the asymmetric unit. This arrangement is consistent with a previous structure of GalNAc-T2 in complex with UDP (PDB entry: 2FFV).[3b] The enzyme structures show the typical GT-A fold located in the N-terminal region and lectin domain located in the C-terminal region (see Figure S2 A). They also feature a flexible loop that can adopt different conformations (see Figure S2 A and discussion below).[3b] A pre-Michaelis complex with UDP-GalNAc and the EA2 peptide, and a ternary complex with UDP and the reaction product (the glycosylated EA2 peptide) were trapped in two of the monomers (see Figure S2 B).

As an alternative strategy to obtain a Michaelis complex, we were encouraged by structural studies of the inverting enzyme OGT[4] to carry out a chemoenzymatic synthesis of UDP-5SGalNAc[5] (Figure S3). The formation of glycosylated peptides was assessed by mass spectrometry (see the Supporting Information). As expected, UDP-5SGalNAc turned out to be a slower substrate than UDP-GalNAc (the specific activity with 2 mM UDP-GalNAc and 0.2 mM ApoCIII peptide was approximately 15-fold higher than the activity with UDP-5SGalNAc; see Figure S4). We also synthesized truncated incompetent EA2 peptides in which the acceptor Thr7 in EA2 was replaced with Cys or Ala (peptide sequences STCPA and STAPA, hereafter named mEA2 peptides). We performed cocrystallization experiments with UDP-5SGalNAc both alone and in combination with EA2 and mEA2 peptides; however, in all cases, we observed only UDP in the active site. Therefore, we conducted soaking experiments (see the Supporting Information) on the basis of the idea that this more rapid process might enable trapping of the complex before catalysis had occurred. Notably, we obtained data at 2.20 and 2.85 Å (see Table S1) that revealed four different complexes within different monomeric units (see Table S2). These monomeric units included the first Michaelis complex structure of GalNAc-T2, containing UDP-5SGalNAc with the mEA2 peptide STCPA (Figure 1), a binary complex containing UDP-5SGalNAc alone, a ternary complex containing UDP and mEA2, and a binary complex with UDP alone (see Figure S2 D). Interestingly, 5SGalNAc was also bound to the lectin domain in some monomers (see Figure S2 E), thus suggesting that hydrolysis of UDP-5SGalNAc took place during the relatively long soaking period. Unlike GalNAc-T10, in which the sugar moiety is located in the β site of the lectin domain,[3a] 5SGalNAc is located in the α site, and is tethered by Asp458, Asn479, Tyr471, and His474 in GalNAc-T2 (see Figure S2 E). This structure explains why Asp458 (the only amino acid that establishes two hydrogen bonds with the sugar moiety) is important for GalNAc–peptide substrate specificity and consequently in tuning the acceptor specificities to define the glycosylation profiles of these enzymes.[6]

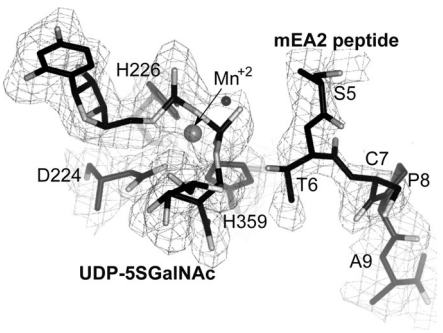

Figure 1. Michaelis complex of GalNAc-T2. Electron-density maps are F_o–F_c syntheses contoured at 2.0 σ for the ligands and 2 F_o–F_c syntheses contoured at 1.0 σ for the residues Asp224, His226, and His359 (see Figure S2 D for a color stereoview).

The enzyme active site shows the typical DxH motif (Asp224-Ser225-His226), which, together with His359, coordinates the manganese atom[3b] in all complexes characterized (Figure 1; see also Figure S5). Specificity for the GalNAc moiety of the donor substrate is defined by several hydrogen bonds with Asp224, Trp331, Gly332, Arg208, Glu334, and Gly308 (see Figure S5). UDP-5SGalNAc overlays well with UDP-GalNAc in all ternary complexes, except the product complex, for which a small displacement of the GalNAc moiety is observed (see Figure S5 D). The methyl group of the acceptor Thr residue is embedded within a hydrophobic pocket formed by Phe280, Trp282, Phe361, and Ala307 (see Figure S5) in both the Michaelis and product complexes. This interaction would be expected to increase the affinity of the enzyme for the acceptor Thr and could explain the preference of GalNAc-T2 for Thr residues.

The NH group of the acetamide moiety and the Trp331 side chain establish hydrogen bonds with a β-phosphate oxygen atom in all ternary complexes (see Figure S5), thus suggesting that these interactions may help define donor substrate specificity and may also facilitate departure. Notably, the hydroxy oxygen atom of the acceptor Thr is quite close to the anomeric carbon atom of the GalNAc moiety in both the pre-Michaelis and the Michaelis complex (O···C1 = 3.8 and 2.5 Å, respectively; see Figure S5 A,B). Furthermore, the Thr oxygen atom of the Michaelis complex is close to two of the phosphate oxygen atoms (2.7 and 3.5 Å), and there is no obvious enzyme residue that could serve as a nucleophile on the other face of the pyranose ring. All these features are most consistent with a front-face type of reaction, in which the phosphate leaving group accepts a proton from the nucleophilic Thr hydroxy group.

As mentioned above, an interesting and intriguing aspect of GalNAc-T2 is the presence of a flexible loop that interacts with the nucleotide-binding site (see Figure S2).[3b,7] This loop, formed by residues Arg362 to Ser373, was previously found to adopt either a closed conformation (see PDB entry 2FFU in Figure S6) to form a lid over UDP, or an open conformation in which the loop folds back to expose UDP to bulk solvent[3b] (see PDB entry 2FFV in Figure 2 A and Figure S6). The open conformation was proposed to facilitate UDP release following catalysis. By taking advantage of the catalytic competence of our crystals, we can conclude that the flexible loop is in a closed conformation when UDP-GalNAc (or UDP-5SGal-

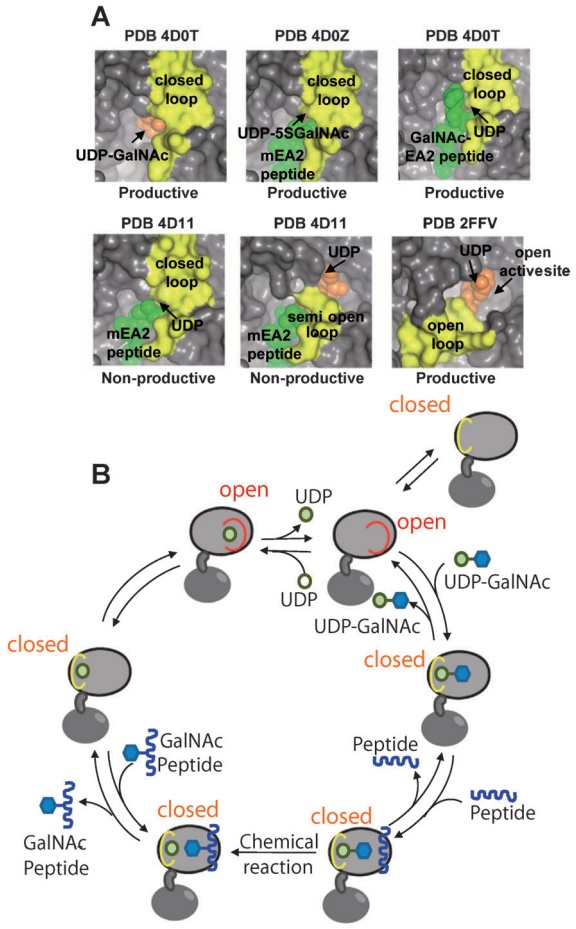

Figure 2. Dynamics of GalNAc-T2 during the catalytic cycle. A) Close-up representation of the surface structures of GalNAc-T2 in complex with substrates and products along the catalytic cycle. B) Proposed ordered kinetic mechanism of GalNAc-T2.

NAc) is bound within the active site, regardless of whether or not the peptide is present (Figure 2A; see also Figure S6). Unlike the structures with the sugar nucleotides, our non-productive ternary complexes with UDP and mEA2 exhibit a mixture of loop conformations (semi-open/closed) that manifests as disorder during analysis of the density maps (Figure 2A; see also Figure S6), thus suggesting that the presence of the GalNAc moiety is important to keep the loop in the closed conformation. These data are most consistent with the opening of the active site, as the loop moves from closed to open to facilitate the release of UDP at the end of the catalytic cycle (Figure 2A). The corollary, which would be the near microscopic reverse, is that the loop must initially be open to bind UDP-GalNAc. Therefore, we conclude that the closed conformation sets the enzyme in a catalytically competent state, whereas the open conformation inactivates the enzyme, although it enables reversible binding of the nucleotide sugar.

The different loop conformations observed in our structures (see Table S2) correlate with two different Trp331 rotameric side-chain positions (see Figure S6B). When the loop is in the closed conformation, Trp331 is tethered by stacking interactions with the GalNAc moiety of UDP-GalNAc, His365, and Phe369. These interactions contribute to keeping the flexible loop closed, thus facilitating further interactions between Tyr367 and the α-phosphate oxygen atom (see Figure S6B). When GalNAc is not present, however, Trp331 can move to a solvent-exposed position, and the flexible loop switches to the open conformation, thus enabling the release of UDP. Overall, our structural data suggest an ordered bi–bi kinetic mechanism for GalNAc-T2 (Figure 2B), as demonstrated for OGT.[4b] This mechanism contrasts with the random sequential mechanism previously proposed for a bovine GalNAc-T in which either the sugar nucleotide or the peptide may bind to the protein in a random manner.[8]

To summarize, within the resting enzyme, the mobile loop initially adopts both open and closed conformations until UDP-GalNAc-Mn^{+2} binds, which causes Trp331 to stack against the sugar and drives the loop to adopt the closed conformation (Figure 2B). A peptide substrate then binds to the enzyme. Subsequently, interactions between the enzyme, UDP-GalNAc, and the peptide substrate enable catalysis to take place, with the active site shielded from water. Following glycosyl transfer, the glycopeptide product departs. At this stage, Trp331 is no longer held in place, and the flexible loop regains mobility between closed and open states, thus permitting the UDP to be released and thereby completing the catalytic cycle. Our proposed mechanism is consistent with a previous experiment in which GalNAc-T2 was purified by using a Muc2 peptide–Sepharose column. The enzyme could only bind in the presence of UDP, and it was only efficiently released upon the removal of UDP.[9]

Although the above structural insight shows the kinetic mechanism and specific interactions within the enzyme active site, it cannot define the precise reaction coordinate and thereby distinguish between mechanistic variations.[10] We therefore performed QM/MM simulations by using the metadynamics approach to define precise details of the glycosyl-transfer reaction for GalNAc-T2 in atomic detail and obtain the free-energy landscape along the reaction coordinate to distinguish between mechanistic variations.[10] The ternary product complex was considered as a starting point (see Figure S7). A combination of classical and QM/MM molecular dynamics was used to equilibrate the enzyme complex, without any restraint (see details in the Supporting Information). Afterwards, the chemical reaction was activated by metadynamics[11] by using three collective variables corresponding to the main covalent bonds undergoing cleavage and formation (see Figure S8). The first collective variable ($C1–O_{Thr}$ distance) measures the formation/cleavage of the glycosidic bond, whereas the second ($C1–O_{UDP}$ distance) describes the formation/cleavage of the sugar–phosphate bond. Finally, the third collective variable (taken as a function of the $O–H_{Thr}$ and $H_{Thr}–O_{UDP}$ distances) measures the extent of proton transfer between the Thr acceptor and the UDP moiety. A detailed description of the reaction can be obtained by following the minimum free-energy pathway on the reconstructed free-energy landscape (see Figure S9) and examining snapshots along this pathway (Figure 3). The Michaelis complex features a hydrogen bond between the acceptor threonine oxygen atom and one of the

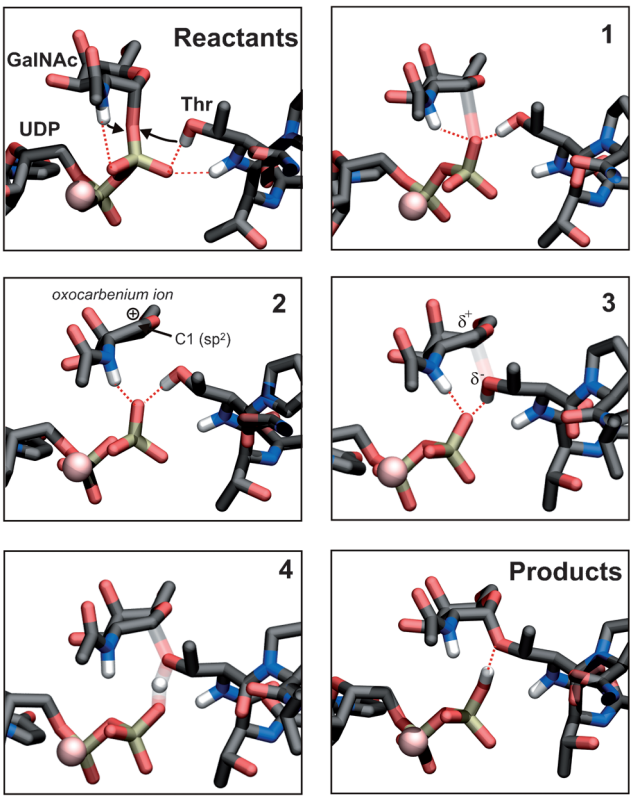

Figure 3. Atomic rearrangement along the reaction pathway. Bonds being broken/formed are drawn as transparent, whereas relevant hydrogen bonds are represented by a dotted red line. Hydrogen atoms have been omitted for clarity, except the acetamido NH group, and the NH and OH groups of the acceptor threonine.

pyrophosphate oxygen atoms. It has often been proposed, on the basis of ternary complexes with substrate analogues[12] or the structural superposition of complexes in which either the sugar moiety or the acceptor is absent,[3b] that the hydrogen atom of the acceptor hydroxy group interacts with the leaving-group oxygen atom of the pyrophosphate moiety. Herein we note that this hydrogen bond forms not with the leaving-group oxygen atom but rather with one of the nonbridging pyrophosphate oxygen atoms. This ground-state interaction makes good chemical sense, since hydrogen bonds are stronger when they are formed between atoms with more closely matched pKa values. This type of configuration, previously proposed on the basis of QM/MM calculations for OtsA,[13] may be common in glycosyltransferases (GTs) operating through a front-face mechanism and underscores the value of analyzing ternary complexes to glean mechanistic insight.

The chemical reaction starts with the elongation of the C–O bond between the UDP and the GalNAc molecule of the donor (the C1–O_{UDP} distance increases by almost 1 Å when going from the reactants to arrangement **1** in Figure 3; see Table S3). Simultaneously, the O_{Thr}–H and N_{acetyl}–H bonds change their hydrogen-bond partners, from a nonbridging phosphate oxygen atom to the bridging oxygen atom, thus placing the hydrogen atom at the proper position to assist the departure of the UDP leaving group. The N_{acetyl}–H···O_{UDP} and O_{Thr}–H···O_{UDP} hydrogen bonds not only stabilize the negative charge being developed at the phosphate group, but they also appropriately position the acceptor molecule to favor the subsequent front-side nucleophilic attack. Therefore, the first part of the reaction can be described as cleavage of the sugar–phosphate bond, assisted by the sugar *N*-acetyl group, together with the formation of a hydrogen bond between the acceptor and the phosphate oxygen atom of the bond being broken.

The sugar—phosphate bond is completely broken in configuration **2** (C1—O_{UDP} = 2.7 Å, Figure 3; see Table S3), which corresponds to a minimum of the free energy landscape (Figure S9). Remarkably, the distance between the donor and the acceptor (C1···O_{Thr}) is still long (> 3 Å), thus suggesting the discrete formation of an oxocarbenium–phosphate ion pair. Further evidence for the change in electronic configuration at the anomeric carbon atom is the shift from a tetrahedral geometry to a trigonal geometry, which is also associated with changes in the conformation of the pyranose ring from a $^4C_1$ chair in the Michaelis complex to a $^4H_3$ half-chair conformation in which the C2, C1, O5, and C5 atoms are almost coplanar (**1**, **2**, and **3** in Figure 3). This change is accompanied by a decrease in the C1–O5 bond length (from 1.38 to 1.27 Å; see Table S3) and an increase in positive charge at the anomeric center (by $-0.40\,e^-$ when going from the reactants to **2**). Both the O_{Thr}–H···O_{UDP} and the N_{GalNAc}–H···O_{UDP} hydrogen bonds contribute to the stabilization of the phosphate–oxocarbenium ion-pair intermediate (**2** in Figure 3), as well as orienting the sugar moiety for the subsequent nucleophilic attack. Afterward, a slight displacement of the GalNAc donor and acceptor molecules takes place to facilitate the interaction between the anomeric carbon atom and the threonine oxygen atom (configuration **3**). Finally, proton transfer to the phosphate group takes place in a process that is almost concomitant with the formation of the sugar–peptide glycosidic bond (Figure 3, configuration **4**).

The simulation shows that cleavage of the GalNAc–UDP bond and the formation of the GalNAc–peptide bond are entirely asynchronous and follow a stepwise pathway. The cleavage of the GalNAc–UDP bond precedes the formation of the GalNAc–peptide bond, and thus an intimate ion-pair intermediate is formed, with the assistance of coordinating hydrogen-bonding interactions between the nucleophilic hydroxy group, the pyrophosphate leaving group, and the *N*-acetyl NH moiety of the electrophilic pyranose group.

The relevance of the acetamido group in catalysis is further supported by the substrate specificity of this family of enzymes, which show a strong preference for UDP-GalNAc and rarely accept UDP-galactose.[14] The overall reaction can be regarded as "a type of internal return", as originally proposed by Sinnott and Jencks in their seminal report on the solvolysis of glucose derivatives[15] by analogy with the S_Ni mechanism for the decomposition of alkyl chlorosulfites.[16] For glycosyl transfer, the names "S_Ni-like" and "S_Ni-type" were later adopted, although the reaction has clear differences from that of alkyl chlorosulfites (the main difference being that the nucleophile is not internal but external). The reaction can also be termed S_N1-type, since an intermediate (although short-lived) is formed. Independently of the

terminology adopted, the reaction mechanism of GalNAc-T2 is consistent with a front-face attack that generates an ion-pair intermediate, as previously found for the retaining GT OtsA, as well as for glucosyl transfer in solution.[13,17]

In summary, we have shown the formation of unprecedented ternary substrate and product complexes of the human retaining GalNAc-T2, which is an enzyme involved in disorders of lipid metabolism and a putative therapeutic target. We combined experimental data with computational studies to provide unique insight into structural features and the mechanism of this important class of isoenzymes, which control protein O-glycosylation. Not only do these snapshots explain the preference of this enzyme for acceptors containing a Thr residue and provide a detailed structural rationale for an ordered bi–bi kinetic mechanism, but they also show that this enzyme constrains reaction components to drive a catalytic mechanism involving front-face attack. We found that the reaction involves a short-lived oxocarbenium ion, which supports this mechanism as likely to be common for most retaining GTs. Finally, the uncovered catalytic mechanism of GalNAc-T2 will serve as a foundation for the design of inhibitors that will serve as useful probe tools and might eventually prove therapeutically useful.

[1] E. P. Bennett, U. Mandel, H. Clausen, T. A. Gerken, T. A. Fritz, L. A. Tabak, *Glycobiology* **2012**, *22*, 736.

[2] C. Steentoft, S. Y. Vakhrushev, H. J. Joshi, Y. Kong, M. B. Vester-Christensen, K. T. Schjoldager, K. Lavrsen, S. Dabelsteen, N. B. Pedersen, L. Marcos-Silva, R. Gupta, E. P. Bennett, U. Mandel, S. Brunak, H. H. Wandall, S. B. Levery, H. Clausen, *EMBO J.* **2013**, *32*, 1478.

[3] a) T. Kubota, T. Shiba, S. Sugioka, S. Furukawa, H. Sawaki, R. Kato, S. Wakatsuki, H. Narimatsu, *J. Mol. Biol.* **2006**, *359*, 708; b) T. A. Fritz, J. Raman, L. A. Tabak, *J. Biol. Chem.* **2006**, *281*, 8613; c) T. A. Fritz, J. H. Hurley, L. B. Trinh, J. Shiloach, L. A. Tabak, *Proc. Natl. Acad. Sci. USA* **2004**, *101*, 15307.

[4] a) M. Schimpl, X. Zheng, V. S. Borodkin, D. E. Blair, A. T. Ferenbach, A. W. Schüttelkopf, I. Navratilova, T. Aristotelous, O. Albarbarawi, D. A. Robinson, M. A. Macnaughtan, D. M. van Aalten, *Nat. Chem. Biol.* **2012**, *8*, 969; b) M. B. Lazarus, J. Jiang, T. M. Gloster, W. F. Zandberg, G. E. Whitworth, D. J. Vocadlo, S. Walker, *Nat. Chem. Biol.* **2012**, *8*, 966.

[5] T. M. Gloster, W. F. Zandberg, J. E. Heinonen, D. L. Shen, L. Deng, D. J. Vocadlo, *Nat. Chem. Biol.* **2011**, *7*, 174.

[6] a) D. J. Gill, K. M. Tham, J. Chia, S. C. Wang, C. Steentoft, H. Clausen, E. A. Bard-Chapeau, F. A. Bard, *Proc. Natl. Acad. Sci. USA* **2013**, *110*, E3152; b) J. Raman, T. A. Fritz, T. A. Gerken, O. Jamison, D. Live, M. Liu, L. A. Tabak, *J. Biol. Chem.* **2008**, *283*, 22942.

[7] A. L. Milac, N. V. Buchete, T. A. Fritz, G. Hummer, L. A. Tabak, *J. Mol. Biol.* **2007**, *373*, 439.

[8] S. Wragg, F. K. Hagen, L. A. Tabak, *J. Biol. Chem.* **1995**, *270*, 16947.

[9] T. White, E. P. Bennett, K. Takio, T. Sørensen, N. Bonding, H. Clausen, *J. Biol. Chem.* **1995**, *270*, 24156.

[10] H. Gómez, R. Rojas, D. Patel, L. A. Tabak, J. M. Lluch, L. Masgrau, *Org. Biomol. Chem.* **2014**, *12*, 2645.

[11] a) A. Laio, M. Parrinello, *Proc. Natl. Acad. Sci. USA* **2002**, *99*, 12562; b) A. Barducci, M. Bonomi, M. Parrinello, *WIREs Comput. Mol. Sci.* **2011**, *1*, 826.

[12] K. Persson, H. D. Ly, M. Dieckelmann, W. W. Wakarchuk, S. G. Withers, N. C. Strynadka, *Nat. Struct. Biol.* **2001**, *8*, 166.

[13] A. Ardèvol, C. Rovira, *Angew. Chem.* **2011**, *123*, 11089; *Angew. Chem. Int. Ed.* **2011**, *50*, 10897.

[14] H. H. Wandall, H. Hassan, E. Mirgorodskaya, A. K. Kristensen, P. Roepstorff, E. P. Bennett, P. A. Nielsen, M. A. Hollingsworth, J. Burchell, J. Taylor-Papadimitriou, H. Clausen, *J. Biol. Chem.* **1997**, *272*, 23503.

[15] M. L. Sinnott, W. P. Jencks, *J. Am. Chem. Soc.* **1980**, *102*, 2026.

[16] E. S. Lewis, C. E. Boozer, *J. Am. Chem. Soc.* **1952**, *74*, 308.

[17] a) J. Chan, A. Tang, A. J. Bennet, *J. Am. Chem. Soc.* **2012**, *134*, 1212; b) J. C. Errey, S. S. Lee, R. P. Gibson, C. Martinez Fleites, C. S. Barry, P. M. Jung, A. C. O'Sullivan, B. G. Davis, G. J. Davies, *Angew. Chem.* **2010**, *122*, 1256; *Angew. Chem. Int. Ed.* **2010**, *49*, 1234; c) S. S. Lee, S. Y. Hong, J. C. Errey, A. Izumi, G. J. Davies, B. G. Davis, *Nat. Chem. Biol.* **2011**, *7*, 631.